

Dark matter in UED : the role of the second KK level

G. Bélanger¹, M. Kakizaki^{1,2}, A. Pukhov³

1) *LAPTH, Univ. de Savoie, CNRS, B.P.110, F-74941 Annecy-le-Vieux, France*

2) *Institute for Theoretical Physics, Hamburg University Luruper Chaussee 149, 22761 Hamburg, Germany*

3) *Skobeltsyn Inst. of Nuclear Physics, Moscow State Univ., Moscow 119992, Russia*

Abstract

We perform a complete calculation of the relic abundance of the KK-photon LKP in the universal extra dimension model including all coannihilation channels and all resonances. We show that the production of level 2 particles which decay dominantly into SM particles contribute significantly to coannihilation processes involving level 1 KK-leptons. As a result the preferred dark matter scale is increased to $R^{-1} = 1.3$ TeV. A dark matter candidate at or below the TeV scale can only be found in the non-minimal model by reducing the mass splittings between the KK-particles and the LKP. The LKP nucleon scattering cross section is typically small, $\sigma < 10^{-10}$ pb, unless the KK-quarks are nearly degenerate with the LKP.

1 Introduction

One of the most attractive explanations to the dark matter(DM) problem is a new weakly interacting particle (WIMP) present in extensions of the standard model. Supersymmetry and extra dimension models are the leading candidates for physics beyond the standard model that also propose a WIMP dark matter candidate. Among the extra dimension models, the UED scenario [1] where all standard model particles are allowed to propagate freely in the bulk is of particular interest. In this model momentum conservation in the extra dimensions entails conservation of KK number. Orbifolding is required to obtain chiral zero modes from bulk fermions, and breaks extra dimensional momentum conservation. However, there remains a discrete subgroup, KK parity, thus the lightest KK-odd particle is stable. In the minimal universal extra dimension model (MUED) the dark matter candidate is in general a vector particle, B^1 , the Kaluza-Klein (KK) level 1 partner of the U(1) gauge boson. One characteristic feature of the model is that the dominant annihilation channels of B^1 are into lepton final states. The observations of PAMELA [2] and Fermi [3] hinting at an excess in the leptonic channel with no counterpart in the antiproton channel has therefore renewed interest in the UED models. Note however that this excess can be explained with astrophysical processes and does not necessarily require a dark matter interpretation [4].

In the MUED model all KK states of a given level have nearly the same mass at tree-level, n/R , where R is the size of the compact dimension. The mass degeneracy is lifted only by standard model (SM) masses. Radiative corrections at the one-loop level further induced mass splittings among level 1 particles, these mass splittings are however small for all weakly interacting particles. This means that co-annihilation channels naturally play an important role in the computation of the relic abundance of dark matter. The relic abundance of B^1 in the MUED model was first computed in [5] and included the

coannihilation of SU(2) singlet KK leptons, the Next-to-Lightest KK particle (NLKP). Apart from the mass difference entering the Boltzmann equation, this calculation was performed in the limit of degenerate masses for all particles at a given KK level. It was shown that the effect of KK-leptons is to increase the dark matter relic abundance. This is because the coannihilation channels are not as efficient as the main annihilation channels, the increase in the number of effective degrees of freedom then induces an increase in the relic abundance contrary to what usually occurs in the MSSM. When the light Higgs mass is large (around 200GeV), the KK-Higgs is the NLKP, coannihilation processes with first KK level Higgs particles lead to a decrease of the relic abundance [6] increasing the preferred mass scale for B^1 dark matter. The relic abundance including all coannihilation channels as well as a precise evaluation of the KK masses were later computed in [7, 8]. The impact of the precise value of the mass splittings between the particles of the first KK level and the LKP was also analysed by going beyond the MUED framework and treating the mass splittings as free parameters. Note that in non minimal UED versions, it is possible to modify the mass splittings by making different assumptions on the boundary terms at the cut-off scale.

At tree-level the second level KK particles have masses twice as large as the ones of the first KK states. It is therefore natural to expect an enhancement of annihilation channels of 1st level KK particles due to the exchange of a s-channel 2nd level KK particle near resonance. For $B^1 B^1$ annihilations, the only potential resonance is the KK partner of the Higgs, h^2 . This particle either decays into $B^1 B^1$ or into standard model particles. It was shown in [9] that the loop-induced decays into standard particles dominate. The inclusion of h^2 in the annihilation processes thus reduces significantly the relic abundance [9, 10]. Other resonance effects occur in coannihilation channels, for example $e^1 e^1 \rightarrow Z^2$. The computation of the relic abundance including all coannihilation channels and level 2 resonances from the Higgs and gauge boson sector was performed in [11]. The effect of level 2 fermions was not included as those particles do not decay dominantly into SM particles. There is however an additional effect from level 2 particles that has been overlooked until now, it is the production of a KK-even level 2 particle in association with a SM particle in the final state. This level 2 particle then decays through loop induced processes into standard model particles. For coannihilation processes where channels with B^2 in the final state are usually kinematically accessible, there can be strong enhancement due to resonance effects from a variety of level 2 particles, for example the coannihilation process $e^1 B^1 \rightarrow e^2 \rightarrow e B^2$ can be strongly enhanced by the contribution of the level 2 lepton. The coannihilation processes can even dominate over the annihilation channels thus reducing the relic density of B^1 .

In this paper we compute the relic abundance of the LKP including all coannihilation channels, all possible level 2 resonances as well as level 2 particles in the final state. We take into account electroweak symmetry breaking effects that were neglected in previous calculations. These will for example impact the masses of the KK-Higgs particles. We consider the case where the DM candidate is the KK partner of the photon, γ^1 , rather than B^1 . Note however that the LKP is dominantly composed of B^1 with only a small W^1 component. The new contributions from annihilation channels into gauge bosons will be suppressed due to this small mixing angle. Finally we include couplings between level-2 gauge or Higgs bosons and standard model fermions. In particular we perform a one-loop computation of the couplings of the level 2 KK-Higgs into quark pairs updating previous calculations [11] by including the contributions from $n = 1$ scalars and weak

gauge bosons. We work first in the context of a minimal UED model¹ then in an extension of the minimal model by treating the mass corrections in the fermion sector as arbitrary parameters. This is done to illustrate the strong dependence of the relic density on mass corrections to the KK states. Indeed the mass corrections influence the coannihilation suppression factor, determine how strongly the channels with level 2 KK-particles in the final state are kinematically suppressed as well as whether the (co)-annihilation process benefits from a resonance enhancement. In the MUED model we find that the mass splitting is such that the second KK level in the final state play an important role. Thus the relic abundance is reduced and the preferred value for the DM mass, consistent with cosmological measurements, $\Omega h^2 = 0.1120 \pm 0.0056$ [13], is shifted above the TeV scale. We also give predictions for direct detection rates and for KK particles production at the LHC.

The paper is organized as follows: in section 2 we briefly present the UED model and give explicit expressions for mass splitting of level 2 particles and loop induced vertices between level 2 and SM particles. In section 3 we discuss DM (co-)annihilation channels and DM observables. In section 4 the results for the relic abundance and the detection rates are discussed. Section 6 contains our conclusions.

2 The UED model

In the UED model all SM fields are upgraded to higher dimensional fields that propagate in the bulk of the flat and finite spatial extra dimensions. Among many space-time structures that can reproduce the SM as a low energy effective theory, we focus on the simplest construction: the five-dimensional space-time with the extra dimension compactified on S_1/Z_2 . Integrating out the extra dimension leads for every 5D field to an infinite tower of 4D Kaluza-Klein modes. In the limit of 5D Lorentz invariance, the mass spectrum of the n^{th} KK modes is n/R , where R is the radius of the compactified dimension. The S_1 compactification destroys the 5D Lorentz invariance, and the Z_2 orbifolding violates 5D momentum conservation. The dispersion relations of 5D particles are modified, resulting in shifts of the KK mass spectrum from n/R and in new decay patterns. The Z_2 orbifolding leads to chiral zero modes (the SM fermions) and removal of the zero modes of the extra dimensional components of the gauge bosons, and allows for 4D brane interactions on the orbifold fixed points. Even though the Z_2 orbifolding violates momentum conservation in the extra dimension, we can retain a parity symmetry under the flip of the fifth coordinate. From the four-dimensional viewpoint, this Z_2 parity prevents mixing between even and odd KK levels, thus guaranteeing the stability of the lightest KK-odd particle, the LKP. The coupling of the KK modes are generated from the 5D Lagrangian after expansion over the KK modes.

We first construct a gauge invariant 5D SM Lagrangian consistent with the above observations. Kinetic terms violating the 5D Lorentz symmetry are compatible with the 5D gauge invariance, and can practically produce the loop-induced mass shifts of the MUED model, as we will see shortly. We consistently implement electroweak symmetry breaking: the vacuum expectation value of the Higgs scalar field is involved not only in

¹Note that our version of the minimal UED model differs slightly from the MUED model of Ref. [12], in particular as concerns the masses of the $n = 2$ gauge bosons and the couplings of level 2 Higgses to SM fermions as detailed in section 2.

the KK electroweak gauge boson and KK fermion mass matrices, but also in the KK Higgs boson mass splitting. In addition, mixing angles caused by electroweak symmetry breaking are taken into account in any interaction term. Gauge-fixing functions and ghost terms are introduced using 5D Goldstone and ghost fields. As far as the bulk 5D Lagrangian is concerned, the KK number is conserved at each vertex. Then, for phenomenological studies, we adjust the KK mass shifts to the MUED ones, which are radiatively generated, and add to our UED model KK-number-violating direct couplings between level 2 particles and SM particles as perturbation because such couplings are necessarily induced at the loop level. The complete description of the Lagrangian and of the gauge fixing procedure is provided in another publication [14]. Here we only describe the mass spectrum including radiative corrections as well as loop induced decays of level 2 particles into pairs of SM particles.

2.1 Mass corrections

The UED model is an effective field theory valid up to a cutoff scale Λ . At loop level mass shifts are introduced by bulk corrections and by localized brane terms. Bulk corrections affect only the gauge bosons KK states while localized brane terms induce mass shifts for all particles. In the minimal UED model one chooses vanishing boundary terms at the cutoff scale. Nevertheless after running down to the electroweak scale radiatively-generated bulk and brane terms affect the mass spectrum lifting the degeneracy of the KK levels. The mass corrections to B^n and W^n were computed in Ref. [12]. The squared mass matrix for neutral gauge bosons reads

$$\mathcal{M}_V^{2(n)} = \begin{pmatrix} (n/R)^2 + m_Z^2 c_W^2 + \delta m_{W^n}^2 & -m_Z^2 c_W s_W \\ -m_Z^2 c_W s_W & (n/R)^2 + m_Z^2 s_W^2 + \delta m_{B^n}^2 \end{pmatrix} \quad (1)$$

where s_W, c_W are the sine and cosine of the weak mixing angle and

$$\delta m_{W^n}^2 = -\frac{5g^2\zeta(3)}{2} \frac{1}{16\pi^4} \frac{1}{R^2} + \frac{15g^2}{2} \frac{n^2}{R^2} \frac{1}{16\pi^2} \log\left(\frac{\Lambda^2}{\mu^2}\right) \quad (2)$$

$$\delta m_{B^n}^2 = -\frac{39g'^2\zeta(3)}{2} \frac{1}{16\pi^4} \frac{1}{R^2} - \frac{g'^2}{6} \frac{n^2}{R^2} \frac{1}{16\pi^2} \log\left(\frac{\Lambda^2}{\mu^2}\right) \quad (3)$$

The renormalization scale μ is chosen to be the mass scale of the 1st KK mode, $\mu = R^{-1}$, and g, g' are the SU(2) and U(1) gauge couplings respectively. The mass of the LKP, γ^1 , is obtained after diagonalisation of the B^1, W^1 mass matrix.

$$\begin{aligned} A_\mu^{(n)} &= W_\mu^{3(n)} \sin\theta_W^{(n)} + B_\mu^{(n)} \cos\theta_W^{(n)}, \\ Z_\mu^{3(n)} &= W_\mu^{3(n)} \cos\theta_W^{(n)} - B_\mu^{(n)} \sin\theta_W^{(n)}, \end{aligned} \quad (4)$$

where $\theta_W^{(n)}$ is the n^{th} level mixing angle which is near 0 for $n \geq 1$. The mass of the LKP is given approximately by the mass of B^1 in Eq. 1 and deviates from $1/R$ at the permil level or less. To take into account the loop corrections to the mass terms in a gauge invariant

manner in the 5D Lagrangian we introduce a correction to the fifth components of the SU(2) and U(1) gauge fields, namely,

$$\mathcal{L}^{5D} = -\frac{1}{4}B_{\mu\nu}B^{\mu\nu} + \frac{Z_B}{2}B_{\mu 5}B_5^\mu + \frac{1}{4}\mathbf{W}_{\mu\nu}\mathbf{W}^{\mu\nu} + \frac{Z_W}{2}\mathbf{W}_{\mu 5}\mathbf{W}_5^\mu \quad (5)$$

This improved tree-level Lagrangian reproduces the loop-corrected mass terms once the parameters Z_B, Z_W are fixed so that the new mass matrix matches Eq. 1, see ref. [14] for a complete description. The gauge boson mass matrix now reads

$$\mathcal{M}_V^{2(n)} = \begin{pmatrix} Z_W(n/R)^2 + m_Z^2 c_W^2 & -m_Z^2 c_W s_W \\ -m_Z^2 c_W s_W & Z_B(n/R)^2 + m_Z^2 s_W^2 \end{pmatrix} \quad (6)$$

As long as m_h is light (near 120GeV), the next to lightest KK particles are the right-handed KK leptons whose mass corrections are also governed by the U(1) coupling. The mass eigenstates are obtained after diagonalisation of the KK lepton mass matrix,

$$\mathcal{M}_l^{(n)} = \begin{pmatrix} n/R + \delta m_{l_L^n} & m_l \\ m_l & -n/R - \delta m_{l_R^n} \end{pmatrix} = \begin{pmatrix} Z_{l_L} n/R & m_l \\ m_l & -Z_{l_R} n/R \end{pmatrix} \quad (7)$$

where the parameters Z_{l_L}, Z_{l_R} describe the loop-improved masses in the tree-level gauge invariant 5D Lagrangian, explicitly

$$\mathcal{L}^{5D} = \bar{\psi}_L i\gamma^\mu D_\mu \psi_L - Z_{l_L} \bar{\psi}_L \gamma^5 D_5 \psi_L + \bar{\psi}_R i\gamma^\mu D_\mu \psi_R - Z_{l_R} \bar{\psi}_R \gamma^5 D_5 \psi_R \quad (8)$$

where $D_{\mu,5}$ are covariant derivatives. In the MUED model, the corrections for the KK partners of singlet leptons read

$$\delta m_{l_R^n} = \frac{9}{4} \frac{g'^2}{16\pi^2} \frac{n}{R} \log\left(\frac{\Lambda^2}{\mu^2}\right). \quad (9)$$

These corrections give a mass splitting at the percent level between the LKP and the NLKP. The mass splittings for the KK lepton doublets and the KK gauge bosons are governed by the SU(2) coupling and are at the few percent level while those for coloured particles are governed by the SU(3) coupling. For the top quark an additional mass splitting is induced by a term proportionnal to the Yukawa coupling. The mass difference between the coloured particles and the LKP are generally large enough (15-20%) that the Boltzmann factor suppresses the contribution of the coloured states in coannihilation channels. To implement the mass corrections for KK-quarks we introduce three new parameters in the Lagrangian $Z_{Q_L}, Z_{d_R}, Z_{u_R}$ and follow the same prescription as for leptons.

In the Higgs sector, the KK charged Higgs $h^{\pm n}$ is the lightest particle, the CP-odd Higgs a^n the next to lightest, and the CP-even Higgs h^n the heaviest at each KK level, the masses read

$$\begin{aligned} m_{h^n}^2 &= \frac{n^2}{R^2} + m_h^2 + \delta m_{H^n}^2 \\ m_{a^n}^2 &= \frac{n^2}{R^2} + m_Z^2 + \delta m_{H^n}^2 \\ m_{h^{\pm n}}^2 &= \frac{n^2}{R^2} + m_W^2 + \delta m_{H^n}^2 \end{aligned} \quad (10)$$

where

$$\delta m_{H^n}^2 = \left(\frac{3}{2}g^2 + \frac{3}{4}g'^2 - \lambda_h \right) \frac{n^2}{R^2} \frac{1}{16\pi^2} \log \left(\frac{\Lambda^2}{\mu^2} \right) \quad (11)$$

where the Higgs quartic coupling, λ_h is related to the mass $m_h = \sqrt{\lambda_h}v$. Since the quartic coupling induces a negative mass correction to the Higgses, for a large value of m_h (and λ_h) the charged Higgs can become the NLKP or even the LKP [6]. In the 5D Lagrangian, corrections to the KK masses of the Higgs doublet ϕ are taken into account by introducing the parameter Z_ϕ

$$\mathcal{L}^{5D} = D^\mu \phi^\dagger D_\mu \phi - Z_\phi D_5 \phi^\dagger D_5 \phi - \mu^2 \phi^\dagger \phi \quad (12)$$

The complete mass corrections in the MUED model are given in Ref. [12]. Note that when computing the spectrum we fix the gauge couplings at the electroweak scale.

2.2 Decays of level 2 particles

At tree-level the $n = 2$ KK-particles can decay either into two $n = 1$ KK-particles or into another $n = 2$ KK particle and a SM one. Both these channels are kinematically suppressed so that the dominant decay mode can be a loop-induced two-body process into SM particles. In particular the $n = 2$ partner of the LKP will decay dominantly into SM fermions. The coupling of γ^2 to standard model fermions is a loop-induced process involving triangle and self-energy diagrams with level 1 fermions and a level 1 gauge boson. The vertices $B^2 \bar{f} f$ and $W^2 \bar{f} f$ have been computed in [12] and are related to the mass corrections from the boundary terms. The dominant loop-induced coupling comes from the level 1 gluon and level 1 quark exchange diagram in the $B^2 q \bar{q}$ vertex. In particular the vertex $B^2 t \bar{t}$ receives corrections that are proportionnal to the top Yukawa, y_t . The loop-corrected vertex reads

$$\begin{aligned} \mathcal{L} = & -\frac{g_1}{\sqrt{2}} \frac{1}{32\pi^2} \log \left(\frac{\Lambda}{\mu} \right) \bar{t} \gamma^\mu \left(Y_{t_L} \left(\frac{7}{24} g'^2 + \frac{27}{8} g^2 + 6g_s^2 - \frac{3}{2} y_t^2 \right) (1 - \gamma_5) \right. \\ & \left. + Y_{t_R} \left(\frac{13}{6} g'^2 + 6g_s^2 - 3y_t^2 \right) (1 + \gamma_5) \right) t B_\mu^2 \end{aligned} \quad (13)$$

where Y_{t_L}, Y_{t_R} are the hypercharge of t_L and t_R . Note that there is a partial cancellation between the gluon and Yukawa contribution. For the light quarks one gets the same expression neglecting the Yukawa term while the couplings to leptons are suppressed as they receive no contribution from gluon exchange nor from large Yukawas. The width of γ^2 is around 1 GeV when $R^{-1} = 1$ TeV and the branching ratios do not vary much with R or ΛR , with 13.9% into $t \bar{t}$, 29.7% into $c \bar{c}$ and $u \bar{u}$, and 8.6% into each of the d-type quarks.

The Higgs bosons, h^2 , a^2 and $h^{2\pm}$, are the other level 2 particles where the dominant decay mode is into SM particles. The level 2 CP-even Higgs, h^2 , predominantly decays into $t \bar{t}$ through the radiatively generated vertex $h^2 t \bar{t}$. The t^1 - g^1 one-loop contribution to the vertex $h^2 t \bar{t}$ is found in Ref. [11]. In addition, we include the vertex corrections from the t^1 - W^1 and t^1 - B^1 one-loop diagrams, as well as the contributions from the kinetic and mass mixings between the level 2 particles and the SM particles on the external legs. The latter contributions stem not only from the gauge interactions but also from the top-Yukawa interaction and Higgs self-interaction, which allow the level 1 Higgs bosons

to run in the loop. The full expression for the vertex $h^2t\bar{t}$ at the one-loop level is given by

$$\mathcal{L} = \frac{y_t}{96\pi^2} \left(16g_s^2 - \frac{39}{4}g^2 + \frac{4}{3}g'^2 - 9y_t^2 + 3\lambda_h \right) \log\left(\frac{\Lambda}{\mu}\right) h^2t\bar{t}. \quad (14)$$

The coefficients of the vertices, $a^2t\bar{t}$ and $h^2t\bar{t}$, have the same form due to gauge invariance. In our analyses, we omit the loop-induced h^2hW -type vertices as such interactions are suppressed by the weak coupling constant. Loop diagrams that involve the Higgs vacuum expectation value are also neglected. Finally the loop induced vertices to lighter quarks, including $\bar{b}b$ are negligible. Given the above interactions, the total decay widths of h^2 ($a^2, h^{2\pm}$) are 395(400,401) MeV for $R^{-1} = 1.3$ TeV, $m_h = 120$ GeV and $\Lambda R = 20$. The branching ratio of each level 2 Higgs boson into the third generation SM quarks is more than 99%.

Notice that in the MUED model the kinetic and mass mixing terms, which contribute to the direct couplings of level 2 particles with SM particles, are proportional to the radiatively-induced mass shifts of the level 2 particles. In the scenarios with arbitrary mass splittings we discuss later, we use the same KK-number-violating interactions as in the MUED model. As long as the arbitrary mass splittings are introduced at the tree level with the cutoff scale fixed as assumed in this paper, only the argument of the logarithm in the KK-number-violating couplings is affected. Since we use the leading log approximation, to take into account such effects is meaningless.

3 Relic abundance

To compute the relic density of dark matter, we have implemented the UED model in CalcHEP [15] and micrOMEGAs2.4 [16, 17]. For this we relied on LanHEP and the new facilities to project the 5D Lagrangian into a 4D one [18]. Implementations of the MUED model in CalcHEP [19] and in FeynRules [20] are available and aim primarily at collider studies. Here, we briefly describe differences between the implementation of our phenomenological UED model and that of the MUED. First, we have implemented the classical 5D SM Lagrangian with the wave function factors, Z_i , which allow for arbitrary mass splittings provided that the mass corrections of KK particles are proportional to n . The Higgs sector and the electroweak symmetry breaking are fully taken into account: for example, the mass splitting among the KK Higgs bosons, Eq.(9), is automatically generated. For simplicity, we neglected the SM quark mixing angles and the renormalization group running of the coupling constants, both of which are included in Ref. [19]. In the realisation of Ref. [20] the level 2 KK-particles are not included as well as the charged and CP-odd level 1 KK-Higgses. Notice that there exist KK Goldstone and ghost fields corresponding to the higher level massive gauge bosons, these were not considered in the preceding implementations. We have implemented both the unitary and the Feynman gauges, and checked that the 5D gauge invariance is retained. The loop induced vertices of the level 2 KK-particles with SM particles described in section 2.2 are then added to the model file by hand, so that the decay widths of the level 2 particles are automatically computed. The model will be described in [14].

To discuss MUED phenomenology, the wave function factors are adjusted to reproduce the loop-induced mass spectrum of the level 1 KK particles: the masses of the higher KK particles are given by integer multiples of those of the level 1 KK particles. In the

MUED model, this holds true for all corrections except the bulk corrections on the gauge bosons, Eqs. 2,3, and those induced by a shift in the renormalization scale. In total, our approximation leads to a shift on the mass of level 2 KK gauge particles less than per-mil for m_{B^2} and 1.2% on the mass of W^2, Z^2 as compared to the MUED case. In comparison, changing the cut-off scale from $\Lambda R = 20$ to $\Lambda R = 50$ leads to 1.6% shifts on these masses. Note however that even a small shift for the mass of a level 2 KK-particle can give rise to a noticeable discrepancy. For example, in most of the parameter space of our model, $\gamma^1 h^{1+} \rightarrow h^{2+} \rightarrow t\bar{b}$ gives the dominant contribution to the relic abundance among loop-induced resonant processes, while $h^{2\pm}$ is light enough that such a pole is not reached at the LKP decoupling temperature in the MUED model, as we will see.

The relic abundance calculation when coannihilation channels are present involve generalizing to the effective annihilation cross section. To display explicitly the dependence on the mass differences we write $\langle\sigma v\rangle$ as

$$\langle\sigma v\rangle = \frac{\sum_{i,j} \langle\sigma v\rangle_{ij} g_i g_j \exp^{-(\Delta m_i + \Delta m_j)/T_f}}{\left(\sum_i g_i \exp^{-\Delta m_i/T_f}\right)^2} \quad (15)$$

where $\langle\sigma v\rangle_{ij}$ is the thermally average cross section for annihilation of any pair of $n = 1$ KK particles into KK-even particles and g_i are the number of degrees of freedom. The Boltzmann suppression factor is $B_i = \exp^{-\Delta m_i/T_f}$ where $T_f \approx m_{\text{LKP}}/25$ and $\Delta m_i = m_i - m_{\text{LKP}}$.

When computing the relic abundance we sum over all $n = 1$ KK particles and include all possible SM particles in the final state as well as the KK-even $n = 2$ particles. Indeed as mentioned above both γ^2 and the level 2 scalar, pseudoscalar and charged Higgs ($h^2, a^2, h^{2\pm}$) decay preferentially into SM particles. Furthermore their decay rate, typical of a weak interaction process, is much faster than the Hubble expansion rate at freeze-out temperatures. These processes therefore contribute to the rate of annihilation of dark matter particles. Other $n = 2$ KK particles, notably KK-leptons, can also be produced in the final state in coannihilation processes. These particles can decay into other $n = 1$ KK states as well as into SM particles. One can show that the contribution of $n = 2$ KK fermions in the final state to the effective annihilation cross section can be taken into account by multiplying their production cross section by the branching fraction of KK fermions into SM particles. We have modified `micrOMEGAs` to take this factor into account. Note however that the contribution of KK leptons in the final state is only at the percent level so this effect is small. The most general case with large branching fractions of heavier level 2 particles into a lighter level 2 particle and a SM particle would necessitate modification of the Boltzmann equation for the computation of the relic abundance. However such cases are not relevant in the UED model under consideration.

We have also checked the consistency of our numerical results for the main annihilation channels with Ref. [7], good agreement was found when we removed the contribution of the level 2 particles coupling to SM particles. Furthermore our results qualitatively agree with [9] when we ignore level 2 particles in the final states (but include h^2 exchange). Some numerical differences are found due to the more accurate computation of the h^2 decay width as described in section 2.2.

The relic abundance calculation can be rather slow in `micrOMEGAs` because of the

very large number of coannihilation channels of the UED model. To avoid computing unnecessary coannihilation channels in the calculation of the contribution of individual channels to the relic abundance we do not include channels for which the Boltzmann suppression factors $B_i B_j < 0.01$ (this is done by setting $B_{eps} = 0.01$ in micrOMEGAs). In the computation of the relic abundance on the other hand we set $B_i B_j < 0.00001$. Note however that setting $B_{eps} = 0.01$ is sufficient to compute Ωh^2 with an accuracy below 1% as we have tested with several input parameters.

4 Results

The minimal UED model contains only three free parameters: R^{-1} , Λ and m_h . We vary the mass scale of KK states in the range 0.4-1.8 TeV. Indirect constraints from electroweak precision observables [21, 22] and rare processes such as $b \rightarrow s\gamma$ [23, 24] set the lower bound between $R^{-1} > 0.4 - 0.6$ TeV while larger values will lead to too much dark matter. We vary $m_h = 114.4 - 300$ GeV to comply with the LEP limit [25] and to include the whole region where the LKP is a neutral particle. For the cut-off scale we choose the range $\Lambda R = 20 - 50$. The upper range for the cut-off scale is motivated by the computation in Ref. [26] of the renormalization group running of the couplings which shows that the U(1) coupling blows up at $E = 50$ TeV when $R^{-1} = 1$ TeV.

For $m_h = 120$ GeV, $\Lambda R = 20$, the value of Ωh^2 computed with only the main annihilation channels shows that $\gamma^1 \gamma^1$ annihilate efficiently and that a rather heavy mass is preferred ($m_{\gamma^1} = 800 - 950$ GeV), see Fig. 1. The dominant channels do not vary much with the scale, for $R^{-1} = 1$ TeV they are into $l\bar{l}$ (19% each), $t\bar{t}$, (21%) $q\bar{q}$ (17% altogether) and $\nu\bar{\nu}$ (3%). The contribution from W,Z boson final states is around $\approx 1\%$ and is suppressed due to the very small $B^1 - W^1$ mixing. The enhancement of the $t\bar{t}$ channel as compared to other quarks is due to the contribution of h^2 . In Fig. 1, we also display the value of Ωh^2 when neglecting the h^2 exchange in s-channel, this is done by removing the loop-induced vertex $h_2 f \bar{f}$. The contribution of h^2 induces roughly a 10% decrease in Ωh^2 as was found previously [9].

Including all coannihilation channels while forbidding the production of γ^2 and other level 2 particles as well as loop-induced couplings between level 2 particles and SM ones leads to an increase in the relic density [5]. This is because the coannihilation cross sections (predominantly those involving the KK partners of singlet leptons) are typically weaker than the ones for $\gamma^1 \gamma^1$ annihilation. Thus the contribution of coannihilation channels, despite that they do not suffer much from a Boltzmann suppression factor, $B_i \approx 0.9$, is more than compensated by the increase in the effective number of degrees of freedom, see Eq. 15. This is in sharp contrast with supersymmetry where coannihilation generally decreases the relic density as the coannihilation channels typically have much larger cross section than the main channel. A large number of coannihilation processes contribute to the effective annihilation cross sections, primarily coannihilation with Higgs, $\gamma^1 H^1 \rightarrow t, \bar{t}(\bar{b})$ as well as a host of other self annihilation processes of the type $l^1 \bar{l}^1 \rightarrow X \bar{X}, H^1 H^1 \rightarrow X \bar{X}', l^1 H^1 \rightarrow X \bar{X}', l^1 V^1 \rightarrow X \bar{X}'$, each individual channel contributing to a small fraction (less than 1%) of the total effective annihilation cross section. Here l stands for e, μ, τ , V^1 stands for W^1, Z^1 and H^1 for any of the neutral or charged Higgs. Coannihilations processes involving quarks are completely negligible. Adding the loop-induced couplings between level 2 KK particles and SM particles has a significant

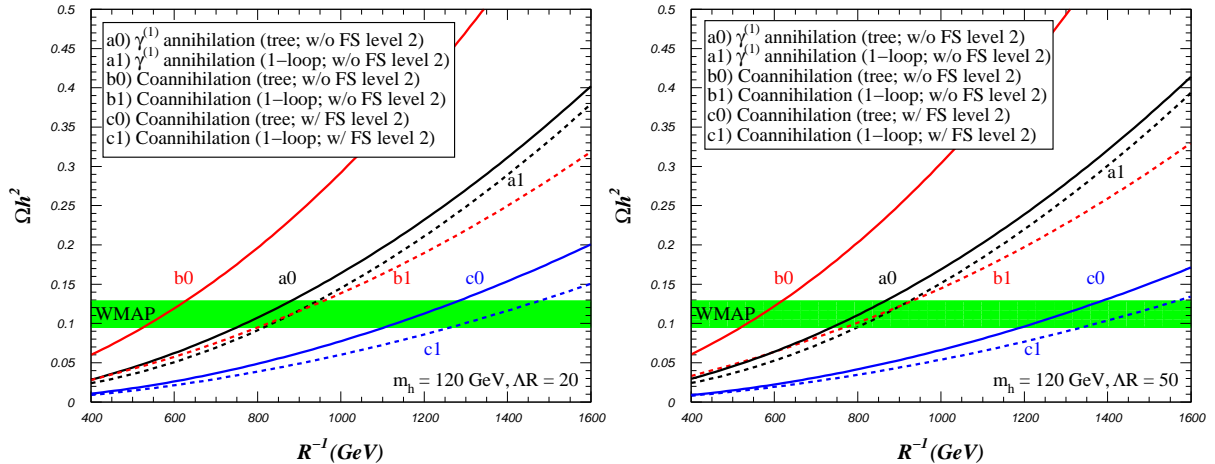


Figure 1: Ωh^2 as function of R^{-1} for $m_h = 120$ GeV, $\Lambda R = 20$ (left) and $\Lambda R = 50$ (right) including different processes as specified on the figure. Here 1-loop stands for one-loop couplings between level 2 and SM particles. The shaded region corresponds to the 3σ preferred region obtained by WMAP [13].

impact on the relic density, see Fig. 1. This is mainly because the new contribution from the process $\gamma^1 h^{1+} \rightarrow h^{2+} \rightarrow t\bar{b}$ benefits from a resonance enhancement thus increasing significantly the effective annihilation cross section. This result depends very sensitively on the mass of the level-2 particle, a small downward shift in the mass, such as in the MUED model used in [11], where the renormalization scale is set to $\mu = 2R^{-1}$ for the level 2 masses, means that the pole effect is avoided at the LKP decoupling temperature. When including the contribution of h^2 and neglecting level 2 KK-particles in the final state, the prediction for the relic abundance is close to the one obtained including only annihilation processes.

When allowing level-2 particles in the final state, mainly γ^2 and $h^2, a^2, a^{\pm 2}$, the relic abundance decreases sharply shifting the preferred value of the DM mass above the TeV scale. This is due to the important contribution of the coannihilation channels ($l^1 \gamma^1 \rightarrow l \gamma^2$) that are enhanced by the exchange near resonance of the $n = 2$ KK singlet lepton. Together these channels make up more than 50% of the (co)annihilation channels. As previously, other coannihilation channels each contribute to a small fraction of the total effective cross section. The contribution of the most important channels is illustrated in Fig. 2, where we have summed the contribution of all leptons in the initial states and all SM particles in the final state. Coannihilation channels involving lepton pairs contribute around 15% and their contribution is comparable to the one of Higgs channels $\gamma^1 H^1$ at large values of R^{-1} . Contributions of the order of a few percent are found for the annihilation channels, $\gamma^1 \gamma^1$, as well as coannihilations of the type $l^1 H^1, H^1 H^1$ or $\gamma^1 l^1$ into only SM particles. This still leaves around 10% contribution from all remaining channels, among these one finds notably channels involving gauge bosons such as $V^1 H^1$ or $V^1 l^1$.

The value of the cut-off scale Λ has an impact on the mass of the KK particles through logarithmic one-loop corrections, Eq. 11. Increasing the scale to $\Lambda R = 50$ leads to heavier KK particles, in particular for KK lepton doublets and KK quarks, and has an impact on Ωh^2 . For example when ignoring the level 2 particles in the final state the contribution of coannihilation channels with KK leptons suffers from a larger Boltzmann suppression factor, this is partly compensated by an increase in the contribution of the h^{2+} pole (as

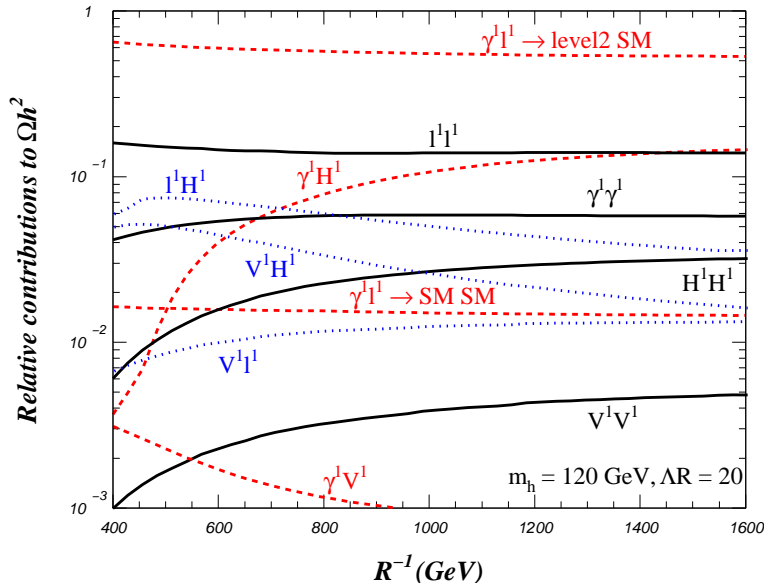


Figure 2: Relative contributions to the relic abundance at the LKP decoupling temperature as a function of R^{-1} for $m_h = 120$ GeV, $\Lambda R = 20$. Here, summation over a class of initial states and all possible final states is performed with the exception of $\gamma^1 l^1 \rightarrow$ level 2 SM which includes only processes with one level 2 particle in the final state and $\gamma^1 l^1 \rightarrow$ SM SM which includes only SM particles in the final state. l^1 stands for $e^1, \mu^1, \tau^1, \nu_i^1$, V^1 for W^1, Z^1 and H^1 for $a^1, h^{1\pm}, h^1$. All remaining channels contribute less than 1%.

well as the one of h^2, a^2) and therefore in the contribution of the coannihilation channels involving Higgs. The net effect is an increase in Ωh^2 by around 5%. On the other hand in the complete calculation including all channels, both the increase in the contribution of the h^{2+} pole and the increase in the pole contribution of KK leptons which dominate the effective cross section lead to a 15% decrease of Ωh^2 . This implies an additional shift of close to 100 GeV in the preferred range for the DM mass.

The value of the light Higgs mass which enters the loop corrections to the KK Higgs masses, has some impact on the prediction of the relic density. Increasing the mass from $m_h = 120$ GeV increases the contribution of coannihilation channels involving level 1 KK Higgses thus reducing Ωh^2 , see Fig. 3. The effect is noticeable only when $m_h > 200$ GeV and is of the order of 7% for $R^{-1} = 1.3$ TeV. For Higgs masses around $m_h \approx 220$ GeV, the charged Higgs becomes the LKP [6].

4.1 Allowing for arbitrary mass splittings

To illustrate the importance of the exact mass splittings between the KK states we generalize our model by allowing additional corrections to the fermion masses. In practice this is done by introducing a small shift in Z_f , Eq. 8. This procedure guarantees that gauge invariance is maintained at the tree-level. This also implies that the relative mass shift is applied to both $n = 1$ and $n = 2$ KK leptons. First we illustrate the effect by modifying only the mass splitting of the KK partners of the lepton singlets, we assume generation universality. The free parameters of the model then include in addition to $\Lambda R, R$ and m_h of the minimal model, five new parameters that affect the masses of the KK fermions, $Z_{l_R}, Z_{l_L}, Z_{Q_L}, Z_{d_R}, Z_{u_R}$.

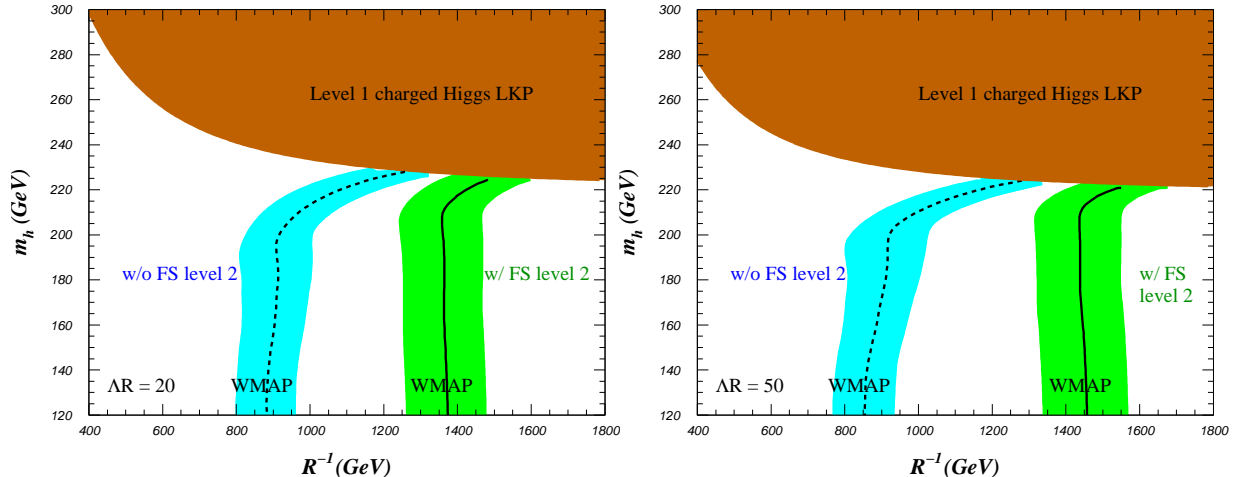


Figure 3: Contour plot of $\Omega h^2 = 0.11$ in the $R^{-1} - m_h$ plane for $\Lambda R = 20$ (left) and $\Lambda R = 50$ (right). The shaded region correspond to the 3σ WMAP range, $0.0952 < \Omega h^2 < 0.1288$, in the case where level 2 KK-particles in the final state are included (dark) or neglected (light grey). All coannihilation channels are taken into account. In the region above the full contour the LKP is the charged Higgs.

We observe, see Fig. 4 for the case of the singlet leptons, that the value of Ωh^2 increases with a smaller mass splitting. This might seem in contradiction with the discussion above since we had argued that the lepton coannihilation had the effect of decreasing Ωh^2 , as seen from Fig.2, a0 and c0. The main effect of a smaller mass splitting is to reduce the contribution of the channel $\sigma(e_R^1 \gamma^1 \rightarrow e \gamma^2)$, indeed the e_R^2 resonance moves very near the threshold for the reaction and so does not contribute significantly to the thermally averaged cross section. This effect is more significant than the increase in the Boltzmann factor which can be at most 15% since in MUED for lepton singlets, $B_{e_R} = 0.86$ for $R^{-1} = 1.3$ TeV. In a sense the relic density is moving towards the value it would have if we had neglected the production of γ^2 in the final state. Conversely an increase in the mass splitting leads to a mild decrease in Ωh^2 , here the Boltzmann suppression of the coannihilation channels is more than compensate by the decrease in the number of degrees of freedom. Note however that the relic abundance is insensitive to the mass splitting if it is more than 3%.

We have also examined the effect of the mass splitting with the partners of the left-handed leptons. The effect follows the same trend although the influence on Ωh^2 occurs for splittings below 5%. The maximum increase in Ωh^2 is comparable to the one obtained for singlet leptons, see the left frame of Fig. 4. Decreasing the mass of KK quarks on the other hand has the opposite effect as for leptons. A smaller mass splitting leads to a lower value for Ωh^2 , this is because in this case the factor B_i changes significantly and QCD processes of the type $q^1 q^1 \rightarrow q q$ give a large contribution. To illustrate this we consider the case where we shift the mass of the KK singlet d-type quarks, see the right frame of Fig. 4. Finally we have also considered the implication of mass shifts for the Higgs. The KK-Higgs masses are modified either by increasing the light Higgs mass or by introducing a mass shift via the parameter Z_ϕ . In both cases this can lead to an increase of Ωh^2 around 10% when the mass difference is a few per-mil.

In summary keeping the mass splitting as a free parameter allows to find scenarios

that have Ωh^2 in the range preferred by cosmological measurements for a lower KK scale. For example for $R^{-1} = 1$ TeV, we find $\Omega h^2 = 0.11$ when $m_{e_R^1} - m_{\gamma^1} = 1.7$ GeV or $m_{e_L^1} - m_{\gamma^1} = 7$ GeV. On the other hand enlarging significantly the mass splittings between the LKP and all level 1 KK particles so as to reduce the contribution of the coannihilation channels would bring us back to the no coannihilation case with a preferred value for the mass of the DM candidate around 800GeV, see Fig. 1.

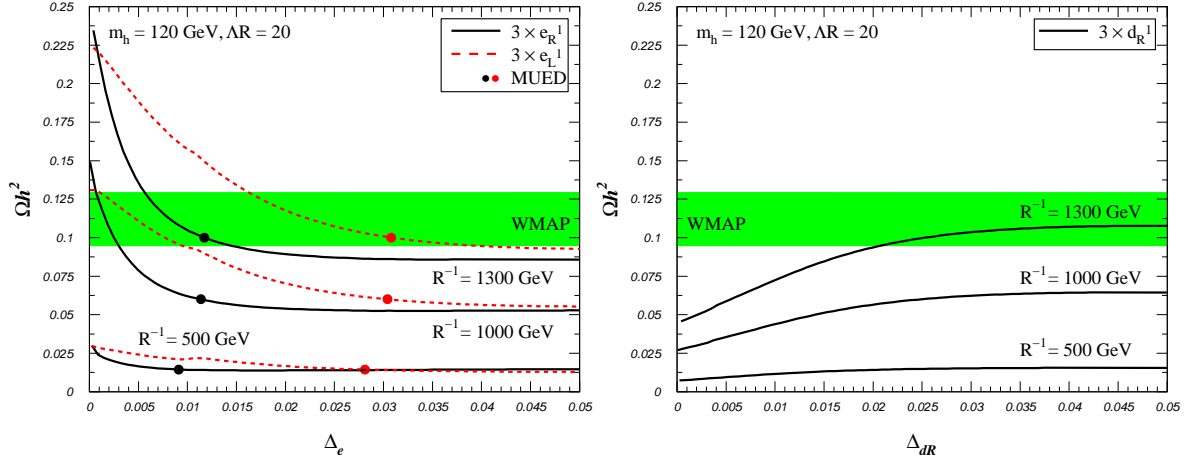


Figure 4: Ωh^2 as function of a) $\Delta_e = (m_{e_R^1} - m_{\gamma^1})/m_{\gamma^1}$ (black) or $\Delta_e = (m_{e_L^1} - m_{\gamma^1})/m_{\gamma^1}$ (red-dot) and b) $\Delta_{dR} = (m_{d_R^1} - m_{\gamma^1})/m_{\gamma^1}$ for $R^{-1} = 0.5, 1, 1.3$ TeV and $m_h = 120$ GeV. The other parameters are as in MUED. Blobs represent MUED points. The shaded region corresponds to the 3σ preferred region obtained by WMAP.

4.2 Dark matter searches

The computation of the LKP-nucleon scattering cross section relevant for direct detection was performed with `micrOMEGAs2.4` [27]. The elastic LKP-nucleon elastic scattering cross section depends both on the Higgs exchange as well as on the diagrams with exchange of level 1 KK-quarks. The amplitude is proportional to $1/m_h^2$ for the first contribution and inversely proportional to the mass difference between the level 1 KK-quarks and the LKP, $1/\Delta^2$ for the second contribution [28]. For the typical mass difference of the MUED scenario, $\Delta = m_{q^1} - m_{\gamma^1} \approx 0.17m_{\gamma^1}$ the Higgs exchange is dominant. When computing the LKP-nucleon cross section we will use the `micrOMEGAs` option that includes the loop contribution to the KK quark exchange diagram. Although this contribution is computed exactly only for scalar particle exchange, it gives a better approximation than the tree-level calculation. Indeed at tree-level one can see the effect of the resonance contribution of the t^1 diagram when R^{-1} is such that $m_q + m_{\gamma^1} = m_{q^1}$. This resonance effect is not physical and is just a sign that including the t-quark contribution by taking into account tree-level diagrams together with a coefficient for describing the t-quark content of the nucleon is not a good approximation [29]. To compute the elastic scattering cross section we use two sets of quark coefficients in the nucleon, the default values of `micrOMEGAs`, $\sigma_{\pi N} = 56, \sigma_0 = 35$ MeV, as well as values extracted from recent lattice calculations $\sigma_{\pi N} = 47, \sigma_0 = 42.9$ MeV. The lattice calculations in particular indicate that the average value for the s-quark operator $\sigma_s = 50$ MeV is lower than expected before [30].

In MUED, cross sections are rather low, typically several orders of magnitude below the best limits of CDMS and Xenon. We compute the rescaled cross section on point-like nucleus [31]. The rescaling factor takes into account the fact that γ^1 does not account for all the dark matter. It is set to $\xi = \Omega h^2 / 0.0945$ when DM is underabundant and to $\xi = 1$ otherwise. Although we display results for scattering on Ge^{76} , the protons and neutrons contribution do not differ much since the contribution from Higgs exchange is dominant, therefore $\sigma_{LKP-Ge} \approx \sigma_{LKP-n} \approx \sigma_{LKP-p}$. The rescaled cross section is rather stable around 1×10^{-10} pb, see Fig. 5 for the default parameters and is reduced by roughly a factor 2 using the lattice coefficients.

In non-minimal models where the mass splittings are treated as free parameters, the LKP-nucleon scattering cross sections can increase by orders of magnitude due to the contribution of the quark exchange diagram which is proportionnal to $1/(m_{q^1} - m_{\gamma^1})^2$ [28]. To illustrate this we decrease the mass of the right-handed d quarks by treating Z_{d_R} as a free parameter. For example for $R^{-1} = 1.3$ TeV and $\Delta m \approx 7$ GeV, we find $\sigma \approx 10^{-8}$ pb, about one order of magnitude below the limit of CDMS [32]. Of course, introducing such a small mass splitting has also an impact on the relic abundance, the new coannihilation channels with KK quarks reduce Ωh^2 as discussed in section 4.1. Note that when the mass splitting becomes very small one can see the effect of the resonance contribution of the b^1 diagram when R^{-1} is such that $m_q + m_{\gamma^1} = m_{q^1}$, this effect is present even using the loop improved calculation.

For $m_h = 220$ GeV, σ_{LKP-N}^{SI} drops by almost one order of magnitude in the MUED case, this is because the Higgs contribution completely dominates. On the other hand the decrease in the cross section with the larger Higgs mass is more modest in the case where Δ_{d_R} is small, see Fig. 5. This is because the Higgs contribution becomes subdominant. The spin dependent cross section is also typically small in MUED, for example $\sigma_{LKP-p}^{SD} = 2.4 \times 10^{-7}$ pb and $\sigma_{LKP-p}^{SD} = 2.4 \times 10^{-8}$ pb for $R^{-1} = 1.3$ GeV. These are almost six orders of magnitude below the current limits [33, 34, 35].

For completeness we have also computed typical cross sections for KK-particles production at LHC with $\sqrt{s} = 14$ TeV. The largest cross sections are obtained for coloured particles. The dominant process are $q^1 q^1$ pairs followed by $q^1 g^1$, both with cross sections in the range $\mathcal{O}(1 - 1)$ pb for the DM preferred mass scale, see Fig. 6. These results are in agreement with previous calculations [36, 37, 38, 39] and are slightly suppressed as compared with the ones obtained using only tree-level KK masses.

5 Conclusion

We have performed a complete computation of the relic density of dark matter in the minimal UED model including all effects of level 2 particle in the intermediate and final state. We have shown that the production of γ^2 in the final state reduces significantly the relic density thus shifting the preferred region from 500-600 GeV to well above the TeV scale (more precisely around 1.3 TeV). The slight tension between the electroweak precision observables which favour $R^{-1} > 600$ GeV [21, 22] for a Higgs mass of 115 GeV and the dark matter observables is thus released. Indeed for $R^{-1} = 1.3$ TeV the contributions to the S and T parameters are suppressed, with in particular $T \approx 10^{-4}$. On the other hand the higher scale means that it will be harder to probe these scenarios at LHC as well as in direct detection. Furthermore because of the important contribution of the coannihilation

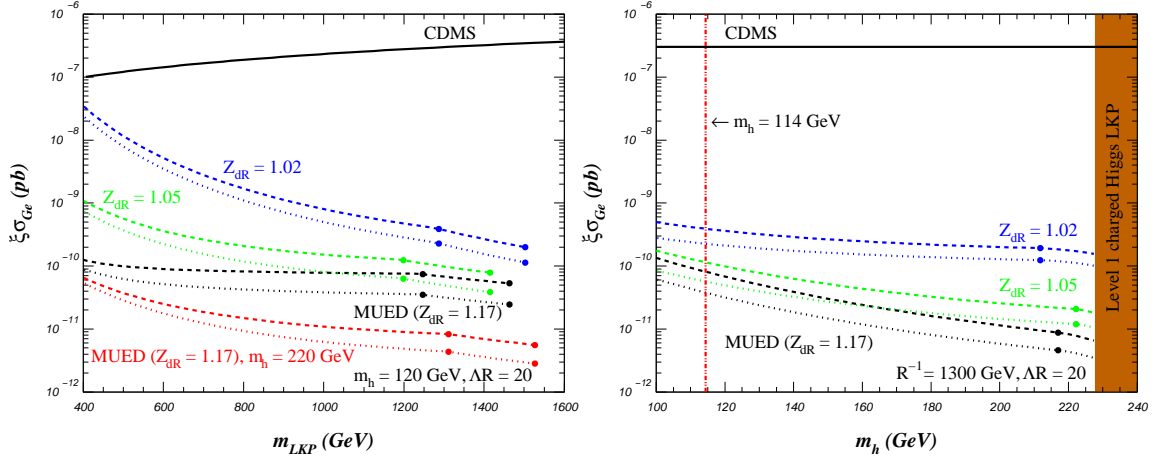


Figure 5: Rescaled LKP-nucleon cross section on Ge^{76} vs m_{LKP} for $m_h = 120$ GeV, $\Lambda R = 20$ and 2 sets of quark coefficients ($(\sigma_{\pi N}, \sigma_0) = (56 \text{ MeV}, 35 \text{ MeV})$ (dash) or $(47 \text{ MeV}, 42.9 \text{ MeV})$ (dot)) and for different values of the mass splitting between the KK singlet d-quarks and the LKP including the MUED case (left panel). The MUED results for $m_h = 220$ GeV are also shown. In each line the region between the blobs is consistent with the 3σ WMAP range. Rescaled LKP-nucleon cross section on Ge^{76} vs m_h for $R^{-1} = 1300$ GeV, $\Lambda R = 20$ (right). In each line the region left of the blob is consistent with the 3σ WMAP range.

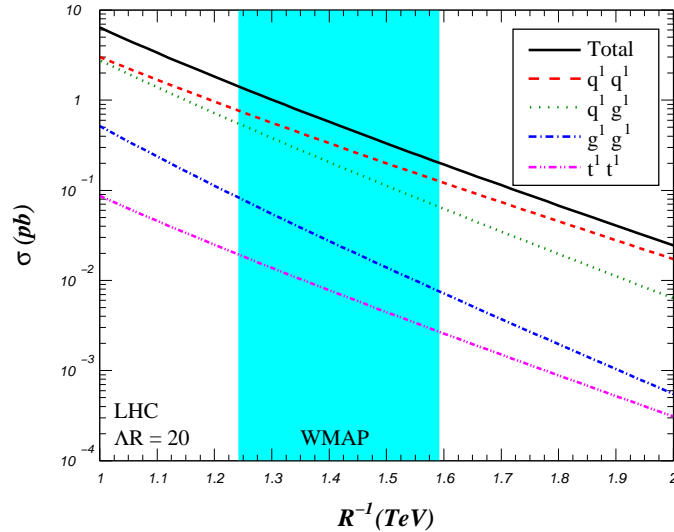


Figure 6: $\sigma(pp \rightarrow q^1 q^1, q^1 g^1, g^1 g^1, t^1 t^1)$ vs R^{-1} at the LHC for $\Lambda R = 20$ using the CTEQ6M PDF's. The K-factor is not included. The shaded region corresponds to the 3σ preferred region obtained by WMAP.

channels, the typical value of $\langle \sigma v \rangle$ relevant for indirect cross section signals is suppressed relative to the typical cross section expected for models that give $\Omega h^2 = 0.1$. Generalizing the model to allow for arbitrary mass shifts in the KK spectrum, we have shown that one could again increase the relic density so that agreement with WMAP was recovered for a LKP around the TeV scale in the case where the lepton NLKP were almost degenerate with the LKP. In this case the direct detection cross section could be strongly enhanced.

We have also shown that these results not only depend sensitively on the mass differ-

ence between the level 1 particle and the LKP but also on the precise mass of the level 2 particles that can be exchanged in s-channel in annihilation or coannihilation processes. In that sense making a precise theoretical prediction of the relic abundance of DM based on collider observables [40] in the event of the observation of KK-particles at the LHC is expected to be extremely challenging. Indeed it would require not only the measurement of the mass and couplings of the LKP but also a precise determination, in some cases better than the percent level, of the masses of level 2 particles. Such precision is not within the reach of the LHC especially for particles that are well above 1 TeV.

6 Acknowledgements

We thank A. Semenov for his help with LanHEP. We also thank A. Belyaev and F. Boudjema for useful discussions. This work was supported by HEPTOOLS under contract MRTN-CT-2006-035505. This work was also supported in part by the GDRI-ACPP of CNRS and by the French ANR project `ToolsDMcoll`, BLAN07-2-194882. The work of AP was supported by the Russian foundation for Basic Research, grant RFBR-08-02-92499-a, RFBR-10-02-01443-a.

References

- [1] T. Appelquist, H.-C. Cheng, and B. A. Dobrescu, *Bounds on universal extra dimensions*, *Phys. Rev.* **D64** (2001) 035002, [[hep-ph/0012100](#)].
- [2] **PAMELA** Collaboration, O. Adriani *et. al.*, *An anomalous positron abundance in cosmic rays with energies 1.5-100 GeV*, *Nature* **458** (2009) 607–609, [[arXiv:0810.4995](#)].
- [3] **The Fermi LAT** Collaboration, A. A. Abdo *et. al.*, *Measurement of the Cosmic Ray $e+$ plus $e-$ spectrum from 20 GeV to 1 TeV with the Fermi Large Area Telescope*, *Phys. Rev. Lett.* **102** (2009) 181101, [[arXiv:0905.0025](#)].
- [4] D. Hooper, P. Blasi, and P. D. Serpico, *Pulsars as the Sources of High Energy Cosmic Ray Positrons*, *JCAP* **0901** (2009) 025, [[arXiv:0810.1527](#)].
- [5] G. Servant and T. M. P. Tait, *Is the lightest Kaluza-Klein particle a viable dark matter candidate?*, *Nucl. Phys.* **B650** (2003) 391–419, [[hep-ph/0206071](#)].
- [6] S. Matsumoto and M. Senami, *Efficient coannihilation process through strong Higgs self-coupling in LKP dark matter annihilation*, *Phys. Lett.* **B633** (2006) 671–674, [[hep-ph/0512003](#)].
- [7] K. Kong and K. T. Matchev, *Precise calculation of the relic density of Kaluza-Klein dark matter in universal extra dimensions*, *JHEP* **01** (2006) 038, [[hep-ph/0509119](#)].
- [8] F. Burnell and G. D. Kribs, *The abundance of Kaluza-Klein dark matter with coannihilation*, *Phys. Rev.* **D73** (2006) 015001, [[hep-ph/0509118](#)].

- [9] M. Kakizaki, S. Matsumoto, Y. Sato, and M. Senami, *Relic abundance of LKP dark matter in UED model including effects of second KK resonances*, *Nucl. Phys.* **B735** (2006) 84–95, [[hep-ph/0508283](#)].
- [10] M. Kakizaki, S. Matsumoto, Y. Sato, and M. Senami, *Significant effects of second KK particles on LKP dark matter physics*, *Phys. Rev.* **D71** (2005) 123522, [[hep-ph/0502059](#)].
- [11] M. Kakizaki, S. Matsumoto, and M. Senami, *Relic abundance of dark matter in the minimal universal extra dimension model*, *Phys. Rev.* **D74** (2006) 023504, [[hep-ph/0605280](#)].
- [12] H.-C. Cheng, K. T. Matchev, and M. Schmaltz, *Radiative corrections to Kaluza-Klein masses*, *Phys. Rev.* **D66** (2002) 036005, [[hep-ph/0204342](#)].
- [13] E. Komatsu *et. al.*, *Seven-Year Wilkinson Microwave Anisotropy Probe (WMAP) Observations: Cosmological Interpretation*, [arXiv:1001.4538](#).
- [14] G. Belanger, M. Kakizaki, A. Pukhov, and A. Semenov. in preparation.
- [15] A. Pukhov, *Calchep 2.3: MSSM, structure functions, event generation, 1, and generation of matrix elements for other packages*, [hep-ph/0412191](#).
- [16] G. Belanger, F. Boudjema, A. Pukhov, and A. Semenov, *micrOMEGAs2.0: A program to calculate the relic density of dark matter in a generic model*, *Comput. Phys. Commun.* **176** (2007) 367–382, [[hep-ph/0607059](#)].
- [17] G. Belanger *et. al.*, *Indirect search for dark matter with micrOMEGAs2.4*, [arXiv:1004.1092](#).
- [18] A. Semenov, *LanHEP - a package for automatic generation of Feynman rules from the Lagrangian. Updated version 3.1*, [arXiv:1005.1909](#).
- [19] A. Datta, K. Kong, and K. T. Matchev, *Minimal Universal Extra Dimensions in CalcHEP/CompHEP*, *New J. Phys.* **12** (2010) 075017, [[arXiv:1002.4624](#)].
- [20] N. D. Christensen *et. al.*, *A comprehensive approach to new physics simulations*, [arXiv:0906.2474](#).
- [21] T. Appelquist and H.-U. Yee, *Universal extra dimensions and the Higgs boson mass*, *Phys. Rev.* **D67** (2003) 055002, [[hep-ph/0211023](#)].
- [22] I. Gogoladze and C. Macesanu, *Precision electroweak constraints on Universal Extra Dimensions revisited*, *Phys. Rev.* **D74** (2006) 093012, [[hep-ph/0605207](#)].
- [23] K. Agashe, N. G. Deshpande, and G. H. Wu, *Universal extra dimensions and $b \rightarrow s\gamma$* , *Phys. Lett.* **B514** (2001) 309–314, [[hep-ph/0105084](#)].
- [24] U. Haisch and A. Weiler, *Bound on minimal universal extra dimensions from $\bar{B} \rightarrow X_s\gamma$* , *Phys. Rev.* **D76** (2007) 034014, [[hep-ph/0703064](#)].
- [25] **Particle Data Group** Collaboration, K. Nakamura *et. al.*, *Review of particle physics*, *J. Phys.* **G37** (2010) 075021.

- [26] G. Bhattacharyya, A. Datta, S. K. Majee, and A. Raychaudhuri, *Power law blitzkrieg in universal extra dimension scenario*, *Nucl. Phys.* **B760** (2007) 117–127, [[hep-ph/0608208](#)].
- [27] G. Belanger, F. Boudjema, A. Pukhov, and A. Semenov, *Dark matter direct detection rate in a generic model with micrOMEGAs2.1*, *Comput. Phys. Commun.* **180** (2009) 747–767, [[arXiv:0803.2360](#)].
- [28] G. Servant and T. M. P. Tait, *Elastic scattering and direct detection of Kaluza-Klein dark matter*, *New J. Phys.* **4** (2002) 99, [[hep-ph/0209262](#)].
- [29] M. Drees and M. Nojiri, *Neutralino-Nucleon Scattering Revisited*, *Phys. Rev.* **D48** (1993) 3483–3501, [[hep-ph/9307208](#)].
- [30] J. Giedt, A. W. Thomas, and R. D. Young, *Dark matter, the CMSSM and lattice QCD*, *Phys. Rev. Lett.* **103** (2009) 201802, [[arXiv:0907.4177](#)].
- [31] G. Belanger, M. Kakizaki, E. K. Park, S. Kraml, and A. Pukhov, *Light mixed sneutrinos as thermal dark matter*, [arXiv:1008.0580](#).
- [32] **The CDMS-II Collaboration**, Z. Ahmed *et. al.*, *Results from the Final Exposure of the CDMS II Experiment*, [arXiv:0912.3592](#).
- [33] E. Behnke *et. al.*, *Improved Limits on Spin-Dependent WIMP-Proton Interactions from a Two Liter CF₃I Bubble Chamber*, [arXiv:1008.3518](#).
- [34] S. Archambault *et. al.*, *Dark Matter Spin-Dependent Limits for WIMP Interactions on 19-F by PICASSO*, *Phys. Lett.* **B682** (2009) 185–192, [[arXiv:0907.0307](#)].
- [35] J. Angle *et. al.*, *Limits on spin-dependent WIMP-nucleon cross-sections from the XENON10 experiment*, *Phys. Rev. Lett.* **101** (2008) 091301, [[arXiv:0805.2939](#)].
- [36] H.-C. Cheng, K. T. Matchev, and M. Schmaltz, *Bosonic supersymmetry? Getting fooled at the CERN LHC*, *Phys. Rev.* **D66** (2002) 056006, [[hep-ph/0205314](#)].
- [37] C. Macesanu, C. D. McMullen, and S. Nandi, *Collider implications of universal extra dimensions*, *Phys. Rev.* **D66** (2002) 015009, [[hep-ph/0201300](#)].
- [38] C. Macesanu, *The phenomenology of universal extra dimensions at hadron colliders*, *Int. J. Mod. Phys.* **A21** (2006) 2259–2296, [[hep-ph/0510418](#)].
- [39] G. Bhattacharyya, A. Datta, S. K. Majee, and A. Raychaudhuri, *Exploring the Universal Extra Dimension at the LHC*, *Nucl. Phys.* **B821** (2009) 48–64, [[arXiv:0904.0937](#)].
- [40] B. C. Allanach, G. Belanger, F. Boudjema, and A. Pukhov, *Requirements on collider data to match the precision of WMAP on supersymmetric dark matter*, *JHEP* **12** (2004) 020, [[hep-ph/0410091](#)].